Alanine-Scanning of the 50's Loop in the *Clostridium beijerinckii* Flavodoxin: Evaluation of Additivity and the Importance of Interactions Provided by the Main Chain in the Modulation of the Oxidation−Reduction Potentials[†]

Mumtaz Kasim and Richard P. Swenson*

Department of Biochemistry, The Ohio State University, Columbus, Ohio 43210

Received July 31, 2001

ABSTRACT: The four-residue reverse turn -Met[56]−Gly−Asp−Glu[59]- in the *Clostridium beijerinckii* flavodoxin provides the majority of the critical interactions with the isoalloxazine ring of the flavin mononucleotide (FMN) cofactor that contribute to the binding and the differential stabilization of its three redox states. Direct side chain contacts include the sulfur-ring interaction of Met56, which primarily influences the oxidized and hydroquinone states, and the hydrogen bond by Glu59 with the N(3)H, which directly (and indirectly through its "anchoring" function) influences all three states to various extents. Involving a novel redox-dependent conformational change, the hydrogen bond formed between the carbonyl group of Gly57 and the N(5)H of the reduced cofactor strongly influences the stability of the semiquinone state. In this study, the sequential elimination of all side chain interactions in various combinations through a systematic alanine-scanning mutagenesis approach was conducted to more completely understand the functional inter-relationships as well as any synergistic interactions that might occur within the loop. In general, additive effects for each side chain on the midpoint potentials for both couples were observed except for the hydroquinone state where some degree of nonadditivity was noted in multiple mutants involving Glu59. The study concluded with the generation of the triple mutant -Ala[56]−Gly−Ala−Ala[59]- in which all side chain interactions are removed. Gly57 was left unchanged because of its critical conformational contribution. Remarkably, this mutant retained the ability to bind the FMN and to thermodynamically stabilize the semiquinone state despite the absence of all side chain interactions. Collectively, these observations emphasize the overriding importance of the *main chain* interactions with the N(5)H of the FMN and the associated redox-dependent conformational change in this loop and leaves little doubt as to its role in the thermodynamic stabilization of the neutral semiquinone state of the FMN cofactor.

The remarkable biochemical versatility of the riboflavin-based cofactor lies in part in the ability of its oxidation−reduction properties to be modulated by the numerous interactions made with the apoflavoprotein. The flavodoxin represents one important class of flavoprotein electron transferase in which this phenomenon has been extensively investigated. These small (≤20 kDa), soluble proteins have been isolated from a variety of microorganisms and eukaryotic algae and contain a single noncovalently bound flavin mononucleotide (FMN)[1] cofactor as their only redox-active component. These rather simple proteins display some of the remarkable characteristics of the flavin, not the least of which is that all three oxidation states of the cofactor—oxidized (OX), one-electron reduced semiquinone (SQ), and two-electron reduced hydroquinone (HQ)—can be observed and studied in these proteins. The thermodynamic stabilization of the neutral form of the SQ in conjunction with the destabilization of the HQ results in very low potentials for the SQ/HQ couple, somewhere in the range of −372 to −512 mV, which are among the lowest potentials observed for flavoproteins (*1*, *2*). These proteins appear to shuttle between these two redox states while participating in various low-potential electron-transfer reactions, without direct involvement of the oxidized form. Another attractive feature of the flavodoxin is that they share significant structural homology with a variety of more complex flavoproteins that function in a myriad of biological reactions, such as cytochrome P450 reductase, cytochrome P450BM-3, and perhaps nitric oxide synthase. Although notable differences in the detailed amino acid sequences occur, even among flavodoxins, many of the interactions made between the apoprotein and the cofactor are generally conserved. Thus, they represent a simplified model in which to investigate structure−function properties that can then be applied to other more complex systems.

A wealth of information on the role played by the protein in perturbation of the potentials of the bound cofactor exists. This includes short- and long-range electrostatic interactions (*3*−*6*), aromatic interactions (*3*, *7*, *8*), sulfur−flavin interactions (*9*), and hydrogen bonding interactions at both N(3)

[†] This study was supported in part by Grant GM36490 from the National Institutes of Health.

* To whom correspondence should be addressed: Department of Biochemistry, 776 Biological Sciences Bldg., The Ohio State University, 484 West 12th Avenue, Columbus, OH 43210-1292.Tel: 614-292-9428; fax: 614-292-6773; e-mail: swenson.1@osu.edu.

[1] Abbreviations: FMN, flavin mononucleotide; OX/SQ, oxidized/semiquinone couple; SQ/HQ, semiquinone/hydroquinone couple.

10.1021/bi011587c CCC: $20.00
Published on Web 10/19/2001

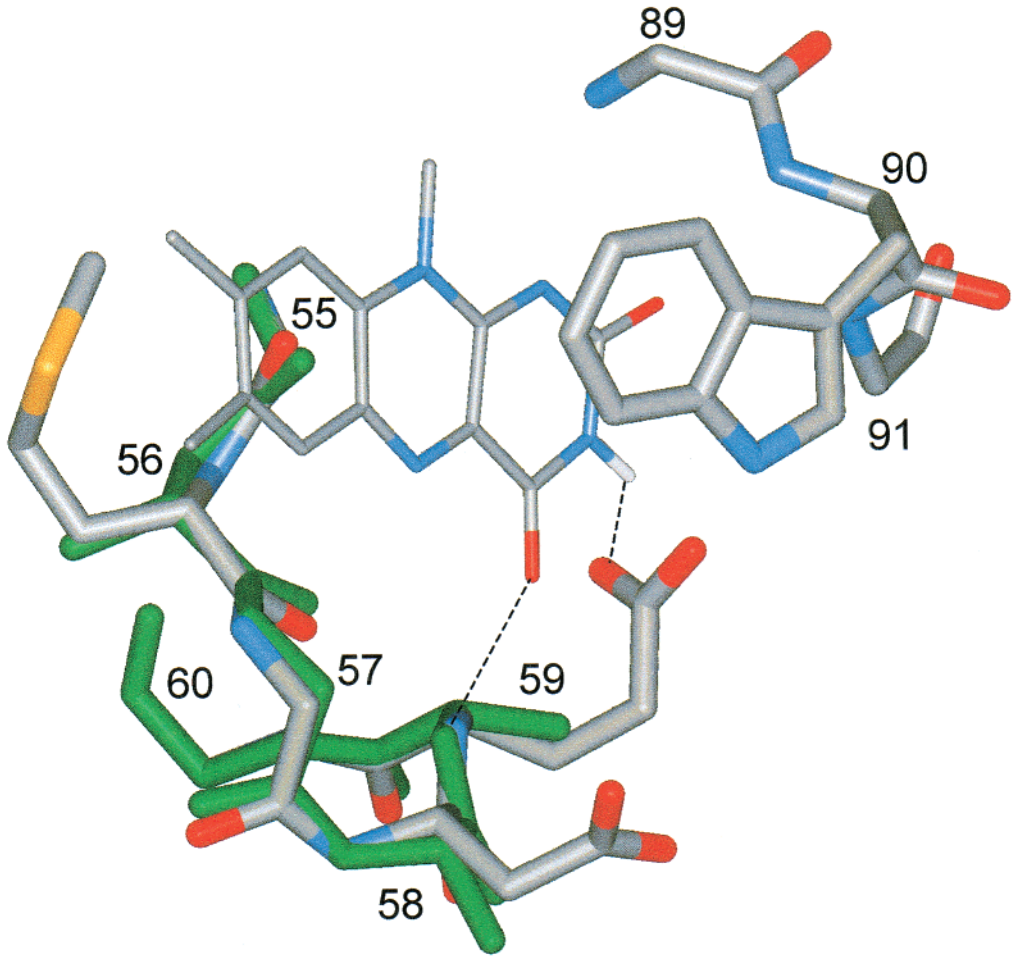

FIGURE 1: Structure of the FMN binding site in wild-type *C. beijerinckii* flavodoxin in the oxidized state showing the major interactions with the isoalloxazine ring. Of note is the *re* face interaction with the side chain of Met56 as well as the *si* face interaction with Trp90. The dashed lines indicate the hydrogen bonding interactions made with the backbone amide and side chain of Glu59. Overlaid in green is the energy-minimized structure of the triple mutant ^{56}AGAA (the loop only). The residues are numbered at the C_α position. The ribityl side chain of FMN, all hydrogen atoms with the exception of N(3)H as well as the side chains of residues 55, 60, 89, and 91 have been omitted for clarity. The wild-type main chain atoms for residue 60 are obscured by the mutant structure due to nearly complete overlap.

(*10*, *11*) and N(5) (*6*, *12*−*14*). Conformational changes that alter flavin protein contacts also make significant contributions as seen in the flavodoxins from *Clostridium beijerinckii* (*12*, *15*, *16*), *Desulfovibrio vulgaris* (*17*, *18*), and *Anacystis nidulans* (*19*, *20*). Many of these interactions have been corroborated and extensively investigated within novel flavin−host model systems (*21*−*23*).

High-resolution crystal structures have been solved for all three oxidation states for the flavodoxin that is isolated from *C. beijerinckii* (MP) and its recombinant form (*12*, *15*, *16*). Of note here is a four-residue surface reverse-turn, the so-called "50's loop", comprised of residues ^{56}MGDE, that contributes many of the crucial interactions made with the isoalloxazine ring of the FMN cofactor (Figure 1). The first residue in the turn, Met 56, flanks the inner or *re* face of the flavin ring, as also seen in the flavodoxins from *C. pasteurianum* and *Megasphaera elsdenii*, which is replaced by either a tryptophan or a leucine in other flavodoxins (*9*, *12*). Mutagenesis studies revealed the importance of sulfur−flavin interactions in the stabilization of the oxidized and destabilization of the hydroquinone states, thus pointing to the functional importance of this residue in maintaining the redox properties of the cofactor (*9*).

Perhaps the most significant distinction of this loop lies in the unusual configuration of the central Gly57−Asp58 peptide bond of the turn. In the oxidized state, this peptide bond exists in the unusual cis conformation with its carbonyl group oriented away from the flavin ring. This conformation, referred to as the "*cis*-O-down" conformation, along with the *trans*-O-down form constitutes about 70% of the observed conformers, with the remainder as the *trans*-O-up form with the orientation of the carbonyl group "flipped" over to point toward the flavin ring (*12*). Reduction of the cofactor results in a structural rearrangement to predominantly the *trans*-O-up conformer. This new orientation brings the carbonyl group in close proximity to the flavin ring such that it can serve as a hydrogen bond acceptor to N(5)H of the reduced FMN. This contributes significantly to the thermodynamic stabilization of the SQ and to a lesser extent the HQ (*12*). Also unique to this flavodoxin is that this structural rearrangement approximates a conversion of a type II β-turn in the OX to a type II′ turn in the reduced states. The functional importance of the Gly57 residue in favoring the type II′ turn as well as the importance of a side chain at position 58 (or position three in the turn) has been established (*12*, *24*). The stability of the turn conformation, which is a direct function of the sequence of the two central residues with the

positioning of the Gly and Ala residues, where Ala represents any amino acid with the exception of glycine and proline, is a prominent feature in the modulation of $E_{ox/sq}$ (*24*). The fourth and final residue of the turn, Glu59, also plays a critical role. Its side chain carboxylate group forms a hydrogen bond "bridge" between the N(3)H of the flavin and the backbone amide of Trp95 and serves to anchor the loop in an optimal orientation in this flavodoxin (*10*, *11*).

The importance of this loop in the modulation of the redox properties of the cofactor is through its direct interaction with the N(5). Substitutions within this loop region have differing effects on structure depending upon the source of the flavodoxin. X-ray crystal structure analysis of the oxidized forms of the Gly61 mutants of *D. vulgaris* flavodoxin, a position homologous to Gly57 of *C. beijerinckii* flavodoxin, revealed that this loop is moved away from the flavin by 5−6 Å (*13*). On the other hand, substitution at the equivalent Asn58 position of *A. nidulans* (*25*) and Gly57 and Asp58 of *C. beijerinckii* (*12*) did not result in any significant structural changes. The only difference noted in the clostridial flavodoxin mutants was the alteration of the conformation of the central peptide bond and the orientation of its carbonyl group, being all *cis*-O-down for Asp58Pro and all *trans*-O-down for Gly57Thr in the oxidized state. While it is understandable for mutations involving this loop region, it is harder to rationalize the effects of more remote mutations when they seem to perturb this loop conformation and therefore the N(5) hydrogen bond strength. Recently, the crystal structures of Y98H and Y98W mutants of the flavodoxin from *D. vulgaris* were solved (*26*). Tyr98 is located in the 90's loop and flanks the *si* face of the flavin, analogous to Trp90 in the clostridial flavodoxins (see Figure 1). Yet, the only structural difference noted in these mutants was the conformation of the 60's loop that had altered resulting in a new orientation of the central carbonyl group. Although the number of flavodoxin mutants has been extensive, the lack of availability of crystal structure information limits our understanding of their effects on the conformation of this loop.

It is therefore of importance to more thoroughly understand all the interactions made by this loop that is adjacent to N(5). However, to date, most of the substitutions involved single amino acid changes. To elucidate any cooperative interactions, especially involving Glu59 since that mutation alone resulted in a disproportionate destabilization of all redox states, a more detailed study involving multiple substitutions within this loop is required. Therefore, this study was initiated to more completely understand the role of this loop and any synergistic relationships among its contributing amino acid residues. All side chain interactions in the loop were sequentially eliminated by alanine-scanning mutagenesis (with exception of Gly57), ultimately resulting in the minimalist sequence, ^{56}AGAA (Figure 1). The use of alanine ensures against large-scale disruptions in main-chain configurations while eliminating the effects of the flavin interactions with each side chain. Gly57 was left as is because of the special structural requirements at this position (*12*, *24*). The results demonstrate the general additivity of mutant effects and also further emphasize the roles of each of the amino acid residues involved. But perhaps the most striking observation is that the mutant lacking all of the side chain interactions provided by this loop was still capable of binding FMN and thermodynamically stabilizing the neutral semiquinone state, a feature characteristic of flavodoxins.

EXPERIMENTAL PROCEDURES

Materials. Anthraquinone-2,6-disulfonate and safranin T were purchased from Fluka Chemicals. Safranin T was recrystallized from ethanol before use. Phenosafranin was obtained from Allied Chemicals. Flavin mononucleotide was extracted from recombinant wild-type *C. beijerinckii* flavodoxin and purified by anion exchange chromatography. All other chemicals were of analytical reagent grade.

Oligonucleotide-Directed Mutagenesis, Protein Expression, and Purification. Mutagenesis was performed using the Kunkel method (*27*). The sequence of the three mutagenic oligonucleotides that were synthesized to generate the mutants were as follows: 5′GCCATGGGCGCTGCAGT-(A)CTCGAGG for ^{56}MGAA; 5′GGTTGCTCTGCCGCGGGC-GATGCAGTTCTCGAGG for ^{56}AGDA; and 5′GCTCTGC-CGCGGGCGCTGCAGT(A)CTCG for ^{56}AGAA.

The underlined bases represent the mutations required for the appropriate amino acid replacements. Screening was facilitated in some cases by the introduction of a unique *Sca*I site by the silent mutation shown in parentheses, by the introduction of a unique *Pst*I site (for the ^{56}MGAA mutant), a *Sac*II site along with the elimination of an *Nco*I site (^{56}-AGDA), and *Pst*I and *Sac*II sites with the elimination of an *Nco*I site (^{56}AGAA). All mutations as well as the sequence integrity of the entire flavodoxin gene were confirmed by automated DNA sequence analysis. All mutants were subcloned into the *Eco*RI and *Hin*dIII sites of the expression vector pKK223-3 for expression in the XL-I Blue strain of *Escherichia coli*. Protein purification proceeded according to established protocols (*3*) except that the proteins were expressed at reduced temperatures to increase the yields of soluble holoprotein. All protein preparations were determined to be >90% pure by SDS−PAGE.

UV−Vis Spectroscopy and Determination of One-Electron Oxidation−Reduction Potentials and FMN Dissociation Constants. All UV−visible spectra were recorded on a Hewlett-Packard HP8452A diode array spectrophotometer. Midpoint potentials were determined as described earlier with all measurements being carried out at 25 °C in 50 mM sodium phosphate buffer at pH 7.0 (*3*, *4*). The indicator dyes used were anthraquinone-2,6-disulfonate ($E_{m,7}$: −184 mV), phenosafranin ($E_{m,7}$: −244 mV), and safranin T ($E_{m,7}$: −280 mV) (all potentials are relative to the standard hydrogen electrode (*28*)). The error in the experimental values reported here are conservatively estimated to be ± 5 mV.

The dissociation constant for the binding of the FMN cofactor to the apoflavodoxin was determined by monitoring the spectral changes accompanying binding under identical experimental conditions used during the determination of the midpoint potentials as described in detail elsewhere (*10*). FMN concentrations were determined using the published extinction coefficient of 12 500 M^{-1} cm^{-1} (*29*). The K_d values for the two reduced states cannot be determined experimentally but were calculated using the thermodynamic equilibria for the various redox states for both free and bound FMN (*30*). The values for the one-electron reduction potentials for free FMN were those determined by Anderson (*31*).

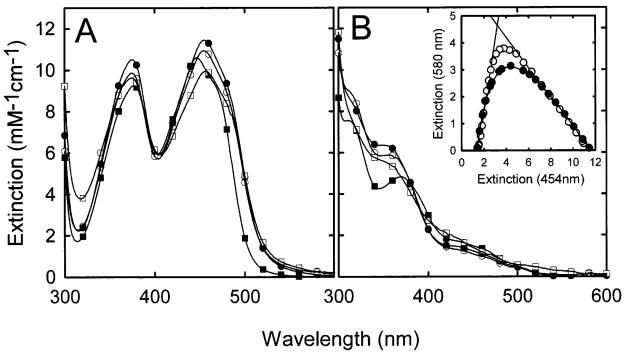

FIGURE 2: UV-vis absorbance spectra for wild-type (closed squares), ^{56}MGAA (open squares), ^{56}AGDA (open circles). and ^{56}AGAA (closed circles) flavodoxins in the oxidized (A) and fully reduced (B) states. The spectra were obtained during a reductive titration with sodium dithionite in a 50 mM sodium phosphate buffer, pH 7.0, at 25 °C. The inset in panel B depicts the spectral changes during the course of the reduction and illustrates the substoichiometric accumulation of the semiquinone species (580 nm) for ^{56}AGDA (open circles) and ^{56}AGAA (closed circles) flavodoxin mutants.

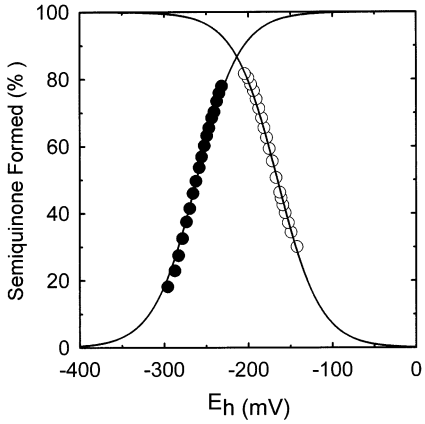

FIGURE 3: Representative oxidation−reduction potential determinations for ^{56}AGDA. The OX/SQ couple (open circles) and the SQ/HQ couple (closed circles) were determined using the indicator dyes anthraquinone-2,6-disulfonate and phenosafranin to establish the system potential (E_h), respectively. In each case, the E_h values are limited by the potential range of each dye. The amount of semiquinone formed is expressed as a percent to facilitate comparison between the two couples. The solid lines are the best fit of the data by nonlinear regression analyses to the Nernst equation, generating midpoint potential values of −165 and −264 mV, respectively.

RESULTS

Characterization of the Double and Triple Mutants. The yields of soluble holoprotein were low as compared to wild type for the ^{56}MGAA, ^{56}AGDA, and ^{56}AGAA mutants. Some of the FMN was found to dissociate during purification, resulting in A_{274}/A_{446} ratios that were higher than wild type (5 to 6 versus 4.4, respectively). This phenomenon is reflective of the significantly higher experimental dissociation constants reported below. The spectral characteristics in all three redox states were recorded during reductive titrations with sodium dithionite under anaerobic conditions. Because of the relatively high dissociation constants of these mutants, at least a 5-fold excess of apoprotein was included in these titrations to ensure that >95% of the FMN was bound. The spectral features of the oxidized species for all mutants differed from wild type with bathochromic shifts of 10, 8, and 8 nm observed for the first transition for ^{56}MGAA, ^{56}AGDA, and ^{56}AGAA, respectively, with concomitant changes in intensity (Figure 2A). An almost complete absence of the characteristic shoulder at 450 nm was striking. The spectral characteristics of the second transition are known to be more sensitive to changes in polarity (*32*). Minor differences in the intensity of the second transition with a slight blue shift in the λ_{max} were also noted, perhaps reflecting only small changes in the solvent exposure of the flavin ring in these mutants. The extinction coefficients for the 450 nm transition were determined to be 9.95 ± 0.25, 10.94 ± 0.6, and 11.45 ± 0.8 mM^{-1} cm^{-1} for ^{56}MGAA, ^{56}AGDA, and ^{56}AGAA, respectively, which are similar to the recombinant wild-type value of 10.6 mM^{-1} cm^{-1} (*33*). The neutral semiquinone species accumulated during the reductive titration of all of the mutant flavodoxins but to a lesser extent than the stoichiometric levels observed for the wild type, reflecting the less stable FMN semiquinone. The spectra of the semiquinone displayed small changes in λ_{max} and intensity, particularly in the 400−500 nm region but were overall similar to wild type. The differences between the hydroquinone spectra of the mutants and also when compared to wild type were more dramatic (Figure 2B). Changes in intensity of the absorbance at 315 nm, 380 nm, and the shoulder at 450 nm are clearly evident. On the basis of model compounds, the wild-type anionic hydroquinone spectrum is characterized by a relatively strong absorbance peak at 380 nm with the flavin in a planar conformation (*32*). The presence of this peak in all of these mutants suggests that a change in ionization state of N(1) is unlikely. Rather, these changes mirror those observed for other flavodoxin mutants and emphasize the sensitivity of the HQ spectrum to slight changes in its environment (*10*, *11*, *24*, *34*). Taken together, all these changes do indicate some degree of structural perturbation in the 50's binding loop in these mutants.

One-Electron Oxidation−Reduction Potentials. The one-electron midpoint potentials were determined in 50 mM sodium phosphate buffer, pH 7.0, at 25 °C in the presence of at least 5-fold excess apoprotein to ensure that all of the FMN remains bound. The system potential at each point in the anaerobic titration was established using suitable redox indicator dyes with established midpoint potential values. All of the titrations were fit to the nonlinear version of the Nernst equation for a single electron reduction. Representative plots of the titration for the OX/SQ and the SQ/HQ couples are shown in Figure 3. The midpoint potential for the OX/SQ couple ($E_{ox/sq}$) for all mutants was more negative than wild type by approximately 70−100 mV (Table 1). The increase for the SQ/HQ couple ($E_{sq/hq}$) was also quite large, being 94 mV for ^{56}MGAA, 135 mV for ^{56}AGDA, and 145 mV for ^{56}AGAA (Table 1). The smaller separation in the potentials for each couple is consistent with the substoichiometric accumulation and the lower stability of the semiquinone species observed during reductive titrations. The role of Met56 in destabilizing the hydroquinone species as reported previously (*9*) was clearly evident on comparison of the $E_{sq/hq}$ values of the various mutants, with ^{56}AGDA and ^{56}AGAA displaying the least negative values, primarily reflective of the more stable hydroquinone species in these mutants.

These results demonstrate that the one-electron reduction potentials of both couples are highly dependent upon the side chain interactions made by both Met56 and Glu59. Particu-

Table 1: Oxidation−Reduction Midpoint Potentials,[a] FMN Dissociation Constants,[b] and Gibbs Free Energy[c] of FMN Binding for Wild-Type and Mutant *C. beijerinckii* Flavodoxins

			K_d					
flavodoxin	$E_{ox/sq}$ (mV)	$E_{sq/hq}$ (mV)	OX (μM)	SQ (nM)	HQ (μM)	ΔG^{OX}	ΔG^{SQ}	ΔG^{HQ}
WT[d]	−92	−399	0.018 ± 0.002	0.0032	0.142	−10.6	−15.7	−9.3
M56A[d]	−72	−331	0.044 ± 0.008	0.0036	0.011	−10.0	−15.6	−10.8
D58A[e]	−93	−380	0.042 ± 0.02	0.0077	0.164	−10.1	−15.2	−9.3
E59A[f]	−186	−298	0.58 ± 0.07	3.97	3.48	−8.5	−11.5	−7.4
MGAA	−189[g]	−305[h]	2.74 ± 0.12	21.0	24.3	−7.6	−10.5	−6.3
AGDA	−165[g]	−264[h,i]	2.84 ± 0.1	8.57	2.0	−7.6	−11.0	−7.8
AGAA	−177[g]	−254[h,i]	2.79 ± 0.11	13.44	2.12	−7.6	−10.7	−7.7

[a] Values are in millivolts at pH 7.0 and 25 °C vs the SHE. [b] The dissociation constants in the oxidized state were measured either by fluorescence or visible spectroscopy and those for the reduced states calculated as described in the text. [c] Values are in kilocalories per mole. [d] From Druhan et al. (*9*). [e] From Kasim et al. (*24*). [f] From Bradley et al. (*11*). [g,h,i] Midpoint potentials were determined using anthraquinone-2,6-disulfonate, safranin T, or phenosafranin as the indicator dye, respectively. All values are an average of at least two independent experiments.

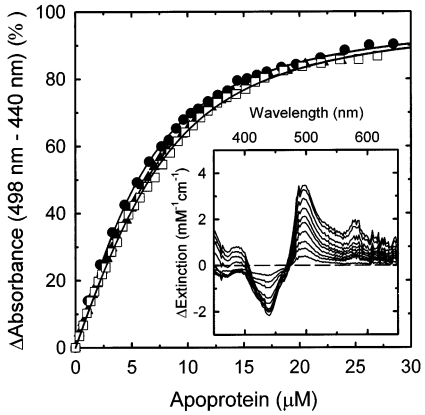

FIGURE 4: Determination of the dissociation constant for the complex between oxidized FMN and mutant apoflavodoxins are shown as follows: ^{56}AGDA (closed circles), ^{56}MGAA (open squares), and ^{56}AGAA (closed triangles). In each case, an FMN solution (~5 μM) in 50 mM sodium phosphate buffer, pH 7.0, at 25 °C was titrated with substoichiometric amounts of freshly prepared apoflavodoxin. After correction for dilution, the changes in extinction coefficients at 440 and 498 nm (inset) associated with complex formation were plotted as a function of the added apoprotein. For clarity, not all difference spectra are shown. The data are shown as a percent change in absorbance to facilitate comparison among the various mutants. The solid lines show the best fit to the data to a single-site binding isotherm.

larly, the ^{56}MGAA mutant has midpoint potentials for both couples that are similar to those of the E59A mutant. Within this context, when the side chain at position 56 is also deleted to yield the ^{56}AGAA mutant, both $E_{ox/sq}$ and $E_{sq/hq}$ shift to less negative values as seen with the M56A substitution relative to wild type (*9*). Similar conclusions can be drawn for the ^{56}AGDA substitution as well. It is worth noting that despite these dramatic shifts in midpoint potentials, the two couples still remain reasonably well separated with $E_{sq/hq}$ being the more negative, resulting from the thermodynamic stabilization of the SQ state.

Changes in FMN Binding. The dissociation constants in the oxidized state were measured by monitoring the spectral changes associated with titrating a known concentration of FMN with increasing amounts of freshly prepared apoprotein under conditions identical to the redox potential determinations (Figure 4). While the K_d values for the semiquinone and hydroquinone forms of the cofactor cannot be measured directly, they can be easily calculated from the linked equilibria that connect the dissociation constants to the determined midpoint potentials as well as to the midpoint potentials of free FMN in solution (*30*). All of the mutants with multiple replacements showed an approximately 150-fold increase in the dissociation constants for the oxidized state (Table 1). The largest changes in K_d for the single substitutions were observed for E59A, which increased by 32-fold (*11*). The K_d values for ^{56}MGAA, ^{56}AGDA, and ^{56}AGAA are all nearly identical and about 5-fold higher than that for E59A. Thus, the removal of the Met56 and/or the Asp58 side chains in this context resulted in a similar loss of binding of the oxidized cofactor as was observed for each individual replacement. It is clear from these results that the hydrogen bonding interaction provided by Glu59 is the most critical interaction in all of these contexts. The semiquinone state was by far the most destabilized by the alanine replacements, with 6570-, 2680-, and 4200-fold increases observed for ^{56}MGAA, ^{56}AGDA, and ^{56}AGAA, respectively. The substitutions in ^{56}MGAA also cause the largest loss in the stability of the HQ, with the K_d increasing 171-fold, whereas the increases for ^{56}AGDA and ^{56}AGAA were 14- and 15-fold, respectively. One of the important observations made for the individual Met56 substitutions previously characterized was that complete or nearly complete elimination of the side chain at this position, represented by the M56G and M56A mutants, bound the HQ state with approximately equal affinity to that of the oxidized state emphasizing the unfavorable sulfur−aromatic interactions that are present in the fully reduced state (*9*). This was accomplished in the M56A mutant by a 14-fold improvement in the binding of the HQ state relative to wild type. It was therefore interesting to note that both ^{56}AGDA and ^{56}AGAA had an approximately 12-fold improvement in the binding of the HQ relative to ^{56}MGAA such that they again bound the HQ with an affinity nearly equal to that for the OX state. Thus, the loss of the interactions provided by the side chains for Asp58 and Glu59 did not significantly affect the sulfur−flavin interaction provided by Met56. This was somewhat surprising, particularly for the loss of the anchoring effect of Glu59. Finally, while all the three redox states have been significantly affected by these mutations, it is obvious that it is the stability of the SQ state that has been affected to the greatest extent by the multiple replacements.

DISCUSSION

Three surface loops provide the majority of interactions with the FMN cofactor in the flavodoxin and related flavoproteins. The "50's loop" in the *C. beijerinckii* flavodoxin provides the largest number of direct interactions

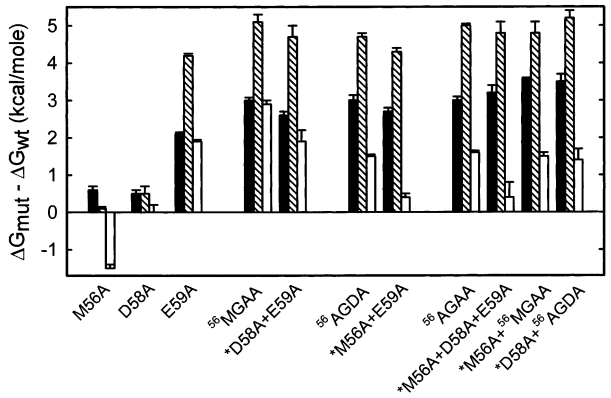

FIGURE 5: Histogram depicting the differences between the binding free energy changes for the FMN cofactor in the oxidized (filled bar), semiquinone (shaded bar), and hydroquinone (open bar) states for the single, double, and triple mutants. All values are relative to the binding free energy for the oxidized cofactor to wild-type flavodoxin. Also shown are the various ways (denoted by a *) in which the individual and double mutants can be added to predict the free energy changes that are observed in the actual multiple mutant.

with the isoalloxazine ring. The principal interactions include *re* face sulfur−flavin contacts involving Met56, hydrogen bonding interaction to N(5)H in the reduced states with the carbonyl group between residues Gly57 and Asp58, hydrogen bonding interaction to C(4)═O with the backbone amide group of Glu59 and the hydrogen bond formed with the side chain of Glu59 to N(3)H. A significant goal has been to thoroughly appreciate the role of this loop in establishing many of the properties of the FMN. The importance of each individual amino acid has been demonstrated during the course of the study of various amino acid replacements at each of these positions (*9*, *10*, *12*, *14*, *24*). It was noted that, with the exception of Glu59, removal of a single molecular contact by a point mutation causes relatively small reductions in the free energy of binding of the cofactor in all oxidation states (Table 1). The fundamental question arises as to whether these interactions act independently or whether synergistic effects are evident. The double mutant analysis approach, which involves pairwise substitutions with alanine at multiple sites, would be useful here because the measured energetic changes can be compared with those of the corresponding single mutations. This should enable the identification of interactions between residues that would normally have been overlooked by single mutations alone. Also, central to this issue is whether it is possible to generate a flavodoxin mutant that can bind flavin despite having none of the side chain interactions made with the 50's loop. If so, what are its properties?

Effects of the Single Substitution within the Context of Multiple Mutations-Methionine 56. The sulfur atom of the methionine side chain makes a weak attractive electrostatic interaction with the electron deficient isoalloxazine ring of the flavin in the oxidized state. As the FMN becomes more electron rich in the fully reduced state, this attractive interaction turns repulsive and contributes to the destabilization of the HQ (*9*). The elimination of the Met56 side chain in the context of the multiple alanine replacements studied here resulted in free energy changes that are entirely consistent with this role of the sulfur atom (Figure 5). Comparison of the free energy changes for the HQ state in ^{56}AGDA and ^{56}AGAA relative to that of ^{56}MGAA reveal that there was an improvement in the binding by 1.5 and 1.4 kcal/mol, respectively. This is comparable to the stability of the HQ state of M56A that is 1.5 kcal/mol greater than wild type. Evidently, the effects of removal of the methionine side chain are noticeable in these multiple mutants and counter the destabilizing effect of the Glu59 mutation. This suggests that the flavin−sulfur interaction was operative even within an altered electrostatic environment and altered flavin binding.

Glutamate 59. Previous studies have demonstrated the importance of Glu59 in the stabilization of the FMN complex in all redox states (*10*, *11*). It is remarkable that the majority of the characteristics of those multiple replacement mutants lacking the Glu59 side chain reflect those of the E59A containing the individual substitution. The λ_{max} for the first transition for all three mutants shows identical shifts to longer wavelengths (454−456 nm) as that of the E59A mutant (*11*). The binding free energy histogram also reveals that the free energy changes for these mutants are dominated by the loss of the interaction(s) provided by Glu59 (Figure 5). These large changes are immediately attributable to the elimination of the donor−acceptor interactions provided by the side chain carboxylate group of Glu59 and possibly to slight alterations between its main chain amide group and the FMN C(4)═O (*11*). Furthermore, the stabilities of the OX and SQ states are very similar among the mutants, which is not surprising if you take into account that the individual Met56 and Asp58 mutations had negligible effects on these oxidation states (Figure 5) (*9*, *24*).

Additivity of Mutational Effects. Our complete understanding of the function of a given amino acid requires knowledge beyond its singular role because its function may also depend on interactions with other residues. The existence of such functionally important interactions between side chains is most convincingly demonstrated by nonadditivity in double-mutant thermodynamic cycles. The sum of the free energy changes of each double mutant are compared with that predicted from the sum of the constituting single mutants in Figure 5. Also shown in the figure are the various ways in which the stabilities of the individual and double mutants can be combined to give the same substitutions as in the triple mutant. The values were additive within experimental uncertainty for all redox states except for the HQ state in some instances. This situation is referred to as simple additivity (*35*) wherein the sum of the free energy changes derived from the single mutations is nearly equal to the free energy change measured in the multiple mutants. What is extraordinary is that it is evident from the free energy histogram (Figure 5) and the correlation plot (Figure 6) that of all redox states, it is the SQ that is the most affected, yet based on the single replacements, the prediction of the free energy changes of the SQ for the multiple mutants is remarkably accurate. Figure 6 plots the free energy changes predicted using various single and double mutant combinations versus the observed free energy changes in the mutants. Additivity would be reflected in data points that lie on the diagonal. A discrepancy of approximately 1.1 ± 0.1 kcal/mol in the estimation of the free energy change for the HQ state was observed, suggesting that perturbations here are not totally additive. Generally, for simple additivity, an error as large as ± 25% has been observed (*35*). Part of this can be attributed to the compounding of errors when summing

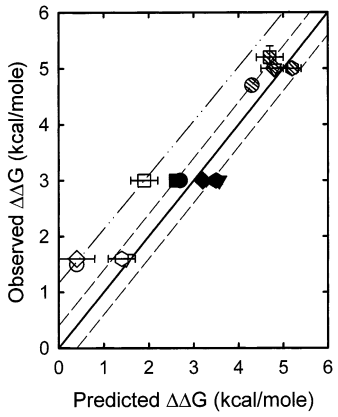

FIGURE 6: Plot of the free energy changes predicted from the constituting single and double mutants versus the actual observed free energy changes for the multiple mutant in the oxidized (closed symbols), semiquinone (shaded symbols), and hydroquinone (open symbols) states. The data for each mutant are represented as follows: ^{56}AGDA (circles), ^{56}MGAA (squares), ^{56}AGAA (diamonds) (all versus the sum of the appropriate single replacements), and ^{56}AGAA (inverted triangle relative to the sum of ^{56}MGAA + M56A) or ^{56}AGAA (hexagons relative to the sum of ^{56}AGDA + D58A). The solid diagonal line represents a totally additive correlation between the values for mutants containing multiple replacements and the summation of the appropriate mutants containing the individual replacements. The dashed lines on either side indicate the limit of uncertainty in the data. The dashed double dot line indicates the observed correlation for the hydroquinone state for which the values fall outside the limit for simple additivity (see text). The values for the triple mutant and the two different summations involving the double mutants (i.e., ^{56}MGAA + M56A and ^{56}AGDA + D58A) fall on the diagonal. Where error bars are not indicated, the errors are commensurate with the relative symbol size.

the single mutants, and the rest is probably due to a weak interaction energy term between the residues that is normally neglected in the summation. A difference of 1.0 kcal/mol translates into a midpoint potential difference of 43 mV, which is well outside the error range of determination. Is it coincidental that the predicted values for the free energy change for all mutants all fall short by a similar amount despite the obvious differences in stability of the HQ state, at least among the double mutants? Given the strong related correlation for these values (the dashed double dot line), we suggest that there is a common reason behind this nonadditivity among all these mutants.

The quantitative effect of a second mutation may be of several types—no effect, antagonistic, partially additive, additive, or synergistic with respect to the first mutation—and this can be extrapolated to higher order mutants as well (*36*). In this particular case, the effects are clearly synergistic because the free energy changes observed in the multiple mutants exceed the sum of the changes in the single mutants. Synergy has been attributed to extensive unfolding of the enzyme and/or to the presence of strain that is introduced by the individual residues with each single mutation being less debilitating as the loss in free energy of binding is compensated partially by the loss in strain (*36*). There is little evidence of extensive unfolding of these mutant structures. Cofactor binding is retained in all cases, and although its affinity is reduced, there was no pattern to this loss among the multiple mutants. In fact, the K_d values are all quite similar. The changes observed in the visible spectrum are rather modest and are not consistent with large changes in the flavin environment. Circular dichroism spectroscopy does not reveal any global disruption of secondary structure (*10*). In terms of strain, it is difficult to rationalize how the surface exposed side chain of Asp58 can introduce any significant strain in the protein. The methionine side chain is also relatively flexible and packs against the isoalloxazine ring with minimal steric interference, ruling out any possibility of strain being introduced here (*9*). Perhaps the anchoring role played by the side chain carboxylate of Glu59 may introduce some degree of strain in the protein, but this alone does not provide an explanation.

The most probable cause for the breakdown of additivity is one that is cited repeatedly in the literature—the mutated residues interact with each other in some manner. However, direct contact among the residues can be ruled out as the sulfur atom of Met56 is situated at a distance that is >10 Å from the carboxyl side chain of Glu59, while the closest approach of the Asp58 side chain to Glu59 is 5.2 Å (*12*). An indirect interaction either through electrostatic interactions or structural perturbations such that the residues no longer behave independently is likely. Since all mutations that showed nonadditivity involved the negatively charged side chain of Glu59, an electrostatic interaction as being the probable cause is conceivable. Nonadditivity in the HQ state alone is not so easily rationalized, but perhaps this interaction exists or is enhanced to a detectable level in the fully reduced anionic state when the N(3)H hydrogen bond interaction is known to be relatively unimportant (*10*, *11*). The fact that summation using ^{56}MGAA+M56A and ^{56}AGDA+D58A results in simple additivity for the HQ state for the triple mutant ^{56}AGAA does indeed indicate that this interaction is already accounted for in the double mutants involving either Met56 or Asp58 (Figure 5 and Figure 6 open inverted triangle and hexagon). In addition, it also provides evidence against any interaction between Met56 and Asp58, which supports the conclusion that the lack of additivity results only from the side chain interaction of Glu59. It should be noted that the lack of the anchoring effect of Glu59 is believed to cause the flavin ring to sit differently in its binding pocket such that the interactions made with the loop are now sufficiently altered. This phenomenon that is present in all mutants could explain the differences in the visible spectra and binding of FMN when compared to wild type. Whether the underlying nature of the interaction responsible for nonadditivity lies in electrostatics or slight structural perturbations is not clear; however, it does seem to involve the Glu59 residue. Further support for this theory comes when substitutions at positions 57 and 58 were considered (data not shown, see also refs *12*, *14*, *24*), where the effects were additive for all three redox states. There are numerous examples of nonadditive effects of double mutations in the literature stressing again that not all residues in proteins act independently and interpretation of the results of single mutations must be done with caution (*36*−*38*)

^{56}AGAA. Special mention must be made of the triple mutant, ^{56}AGAA. In this mutant, all the side chain interactions provided by this loop are essentially eliminated through their replacement with alanine while maintaining the main chain configuration through the retention of the crucial structural characteristics provided by Gly57 (*12*, *24*). Surprisingly, these rather drastic alterations did not preclude FMN binding. Furthermore, despite the 3 kcal/mol loss in

binding free energy for the oxidized cofactor and the elimination of nearly all the side chain interactions with the isoalloxazine ring, the neutral FMN SQ is still substantially thermodynamically stabilized and the two redox couples remain reasonably well separated. As the site of the conformational change is relatively intact in ^{56}AGAA (and all the other mutants), the changes in midpoint potentials observed are the direct result of the loss of side chain interactions with Met56 and Glu59. A distortion in the N(5) interaction cannot be ruled out due to the removal of the Glu59 side chain; however, the extent of disruption would likely be uniform for all these mutants, including the E59A mutant. Main chain configurations for the turn likely have not been substantially altered given the ability of the protein to bind FMN, which displays some of the characteristic spectral qualities as the wild type. Molecular modeling and computational studies also support this conclusion (Figure 1) [data not shown].

The one remaining isoalloxazine ring/side chain interaction in the ^{56}AGAA mutant is with the *si*-face aromatic residue, Trp90 (Figure 1). For another study, this residue was independently replaced with alanine. It was observed that despite the approximately 30-fold increase in the dissociation constant for the oxidized FMN, the midpoint potential for the OX/SQ couple for W90A was only marginally affected by this replacement, again demonstrating that aromatic−flavin interactions do not seem to play a major role in the preferential stabilization of the SQ [unpublished results and ref *3*]. In fact, we entertained the notion of generating the ^{56}AGAA/W90A quadruple mutant for which *all* side chain interactions with the flavin ring are eliminated. However, based on the observed dissociation constants for ^{56}AGAA and W90A, it was thought that this protein would bind FMN too weakly for meaningful biochemical characterization, so it was not produced. Nonetheless, collectively, these observations emphasize the overriding importance of the *main chain* interactions with the N(5)H of the FMN and the associated conformational change in this loop that occurs during the reduction, especially in the thermodynamic stabilization of the neutral SQ state. These studies can now leave little doubt of this fact, which was a very early and insightful observation for this group of proteins (*15*).

REFERENCES

1. Mayhew, S. G., and Tollin, G. (1992) in *Chemistry and Biochemistry of Flavoenzymes* (Müller, F., Ed.) pp 389−426, CRC Press, Boca Raton, FL.
2. Ludwig, M. L., and Luschinsky, C. L. (1992) in *Chemistry and Biochemistry of Flavoenzymes* (Müller, F., Ed.) pp 427−466, CRC Press, Boca Raton, FL.
3. Swenson, R. P., and Krey, G. D. (1994) *Biochemistry 33*, 8505−14.
4. Zhou, Z., and Swenson, R. P. (1995) *Biochemistry 34*, 3183−92.
5. Chang, F. C., and Swenson, R. P. (1997) *Biochemistry 36*, 9013−21.
6. Hoover, D. M., Drennan, C. L., Metzger, A. L., Osborne, C., Weber, C. H., Pattridge, K. A., and Ludwig, M. L. (1999) *J. Mol. Biol. 294*, 725−43.
7. Zhou, Z., and Swenson, R. P. (1996) *Biochemistry 35*, 15980−8.
8. Lostao, A., Gomez-Moreno, C., Mayhew, S. G., and Sancho, J. (1997) *Biochemistry 36*, 14334−44.
9. Druhan, L. J., and Swenson, R. P. (1998) *Biochemistry 37*, 9668−78.
10. Bradley, L. H., and Swenson, R. P. (1999) *Biochemistry 38*, 12377−86.
11. Bradley, L. H., and Swenson, R. P. (2001) *Biochemistry 40*, 8686−95.
12. Ludwig, M. L., Pattridge, K. A., Metzger, A. L., Dixon, M. M., Eren, M., Feng, Y., and Swenson, R. P. (1997) *Biochemistry 36*, 1259−80.
13. O'Farrell, P. A., Walsh, M. A., McCarthy, A. A., Higgins, T. M., Voordouw, G., and Mayhew, S. G. (1998) *Biochemistry 37*, 8405−16.
14. Chang, F. C., and Swenson, R. P. (1999) *Biochemistry 38*, 7168−76.
15. Burnett, R. M., Darling, G. D., Kendall, D. S., LeQuesne, M. E., Mayhew, S. G., Smith, W. W., and Ludwig, M. L. (1974) *J. Biol. Chem. 249*, 4383−92.
16. Smith, W. W., Burnett, R. M., Darling, G. D., and Ludwig, M. L. (1977) *J. Mol. Biol. 117*, 195−225.
17. Watenpaugh, K. D., Sieker, L. C., and Jensen, L. H. (1976) in *Flavins and Flavoproteins: Proceedings* (Singer, T. P., Ed.) pp 405−410, Elsevier Scientific, Amsterdam, New York.
18. Watt, W., Tulinsky, A., Swenson, R. P., and Watenpaugh, K. D. (1991) *J. Mol. Biol. 218*, 195−208.
19. Laudenbach, D. E., Straus, N. A., Pattridge, K. A., and Ludwig, M. L. (1988) in *Flavins and Flavoproteins, 1987: Proceedings of the Ninth International Symposium on Flavins and Flavoproteins, Atlanta, Georgia, USA, June 7−12, 1987* (Edmondson, D. E., and McCormick, D. B., Eds.) pp 249−260, W. de Gruyter, Berlin.
20. Luschinsky, C. L., Dunham, W. R., Osborne, C., Pattridge, K. A., and Ludwig, M. L. (1991) in *Flavins and flavoproteins 1990: Proceedings of the Tenth International Symposium, Como, Italy, July 15−20, 1990* (Curti, B., Ronchi, S., and Zanetti, G., Eds.) pp 409−413, W. de Gruyter, Berlin, New York.
21. Breinlinger, E. C., and Rotello, V. M. (1997) *J. Am. Chem. Soc. 119*, 1165−6.
22. Cuello, A. O., McIntosh, C. M., and Rotello, V. M. (2000) *J. Am. Chem. Soc. 122*, 3517−21.
23. Goodman, A. J., Breinlinger, E. C., McIntosh, C. M., Grimaldi, L. N., and Rotello, V. M. (2001) *Org. Lett. 3*, 1531−4.
24. Kasim, M., and Swenson, R. P. (2000) *Biochemistry 39*, 15322−32.
25. Drennan, C. L., Pattridge, K. A., Weber, C. H., Metzger, A. L., Hoover, D. M., and Ludwig, M. L. (1999) *J. Mol. Biol. 294*, 711−24.
26. Reynolds, R. A., Watt, W., and Watenpaugh, K. D. (2001) *Acta Crystallogr. D Biol. Crystallogr. 57*, 527−535.
27. Kunkel, T. A. (1985) *Proc. Natl. Acad. Sci. U.S.A. 82*, 488−92.
28. Clark, W. M. (1972) *Oxidation−Reduction Potentials of Organic Systems*, Robert E. Krieger Publishing Company, Huntington, NY.
29. Whitby, L. G. (1953) *Biochem. J. 54*, 437−442.
30. Dubourdieu, M., le Gall, J., and Favaudon, V. (1975) *Biochim. Biophys. Acta 376*, 519−32.
31. Anderson, R. F. (1983) *Biochim. Biophys. Acta. 722*, 158−62.
32. Müller, F. (1991) *Chemistry and Biochemistry of Flavoenzymes*, Vol. 1, CRC Press, Boca Raton, FL.
33. Eren, M. (1990) Ph.D. Thesis, The Ohio State University, Columbus, Ohio.
34. Lostao, A., El Harrous, M., Daoudi, F., Romero, A., Parody-Morreale, A., and Sancho, J. (2000) *J. Biol. Chem. 275*, 9518−26.
35. Wells, J. A. (1990) *Biochemistry 29*, 8509−17.
36. Mildvan, A. S., Weber, D. J., and Kuliopulos, A. (1992) *Arch. Biochem. Biophys. 294*, 327−40.
37. Ohmae, E., Iriyama, K., Ichihara, S., and Gekko, K. (1998) *J. Biochem. (Tokyo) 123*, 33−41.
38. Zhang, X. J., Baase, W. A., and Matthews, B. W. (1991) *Biochemistry 30*, 2012−7.

BI011587C